High fluorescent water soluble CdTe quantum dots-a promising system for light harvesting applications

Arsenio de Sa • Isabel Moura • Ana S. Abreu • Manuel Oliveira - Miguel F. Ferreira Ana V. Machado

Abstract

The entrapment of quantum dots (QDs) in the inner part of micelles formed by surfactant polymers is a powerful methodology to prepare stable and photoluminescent core nanoparticles with enhanced optical properties. These features are crucial for the application of QDs in the design of hybrid assemblies for light harvesting applications, where energy transfer processes are required. The present work was focused on the synthesis of a surfactant homopolymer, poly (acrylic acid) (PAA) macroRAFT, to be used as a stabilizer of hydrophobic cadmium telluride (CdTe) QDs in aqueous solution. PAA macroRAFT was synthesized by reversible addition-fragmentation chain-transfer (RAFT) polymerization in a single chemical reaction. Its micelles were used to entangle and entrap hydrophobic CdTe QDs, with different molar ratio of polymer and QDs. The morphology and optical properties of the entrapped QDs were determined. The results showed that PAA macroRAFT is able to form micelles with a critical micelle concentration of 2.08mg/mL. It was also noticed that the molar ratio of polymer and QDs have high influence on the QDs' morphology and their optical properties. The QDs' photoluminescence quantum yield was enhanced approximately 23% upon their entrapment in PAA macroRAFT micelles, using 60 equivalents of polymer. Moreover, while in solution, QDs are well-dispersed, having a 3.5 nm diameter, upon being entrapped in the micelles, tend to form clusters with a size around 100 nm .

Keywords Amphiphilic polymer · RAFT polymerization · Water soluble quantum dots · Enhanced photoluminescence • Polymer-coated QDs

Introduction

Intelligent materials constitute an attractive research field among the scientific community. Many efforts are being performed in the development of new methodologies and strategies to take advantage of renewable energy, including the design of assemblies to build up artificial light-harvesting systems (Ramachandra et al. 2011). Its development has motivated the interest in photoluminescent semiconductor nanoparticles (NPs) to achieve efficient, cost-effective light energy

conversion and storage materials (Snaith 2013). These NPs, also known as semiconductor quantum dots (QDs), can be important building blocks in the production of advanced materials, such as light harvesters, due to their unique dimensions, size-dependent physicochemical properties, high extinction coefficients, low cost, and the possibility of hot electron injection, as well as multiple exciton generation (Hoffman et al. 2014; Zhou et al. 2011). Typically, in artificial antenna systems, the components are well-organized and covalently linked or assembled by multiple noncovalent interactions (Ramachandra et al. 2011). Particularly, cadmium telluride (CdTe) QDs are one of the most widely used QDs, owing to their quantum effect of the electron confinement and their emission wavelengths span the entire visible light spectrum (Viet Ha et al. 2012). Nevertheless, it is essential to stabilize the QDs with a capping layer, so they can retain their optical properties for longer times. Frequently, when the QDs' capping layer is not suitable for a given application, it is essential to replace it. However, such replacement often results in the reduction of the NPs' photoluminescence quantum yield (PLQY) (Haibing et al. 2007). A strategy that can be used to avoid replacing the capping layer consists in the entrapment of the NPs within a shell, as a second capping layer. The latter interacts with the original capping layer and allows the QDs to retain or enhance their optical properties (Yu et al. 2006). One example of this approach is the entrapment of QDs stabilized with hydrophobic ligands in the inner part of micelles (Yuwen et al. 2011). Micelles can be formed either by low molecular weight (LMWS) (Haibing et al. 2007) or polymeric surfactants (Yu et al. 2006). The main advantage of using polymeric surfactants is related to their ability to form micelles at lower concentrations when compared to LMWS (Ahmad et al. 2014); thus, less amount of material is required.

Yuwen et al. (2011) used octadecylamine-modified poly (acrylic acid) (PAA-ODA), a surfactant polymer, to entrap hydrophobic CdTe/CdS core/shell and produce water soluble systems. The authors observed a PLQY enhancement when QDs were entrapped by the PAAODA micelles. Haibing et al. (2007) also reported an enhancement of PLQY when CdSe/ZnS core/shell QDs were entrapped by micelles formed by a gemini surfactant.

The present work aims to develop a water soluble fluorescent system, based on hydrophobic CdTe QDs entrapped by micelles of a surfactant homopolymer,

PAA macroRAFT, with potential application in the photoelectronic field. PAA macroRAFT was synthesized by reversible addition-fragmentation chain-transfer (RAFT) polymerization, which allowed us to produce in a single chemical reaction a homopolymer with surfactant capacity. The synthesis and characterization of PAA macroRAFT, its ability to entrap hydrophobic CdTe QDs capped with 1-dodecanethiol (CdTe-DDT), and its influence on the QDs' PLQY will be presented and discussed.

Experimental section

Materials

Tellurium powder (200 mesh, 99.99%) and cadmium chloride anhydrous ($CdCl_2$, 99.99%) were purchased to Alfa Aesar. 2-cyano-2-propyl dodecyl trithiocarbonate (CTA, 97%), acrylic acid (AA, 99%), 2,2'-azobis(2methylpropionitrile) (AIBN, 98%), 1-dodecanethiol (1DDT, ≥ 98%), and 8-anilino-1-naphthalenesulfonic acid ammonium salt (ANS, ≥ 97%) were acquired from Sig-ma-Aldrich. Mercaptoacetic acid (MAA, 97%), methanol (MeOH,

99.9%), ethyl ether (99%), tetrahydrofuran (THF, 99.9%), chloroform (99.9%), and acetone (99.9%) were obtained from Fisher Chemical. Sodium borohydride ($NaBH_4$, 98%), sodium hydroxide (NaOH), and deuterated dimethyl sulfoxide ($DMSOd_6$) were bought to Acros Organics. All chemicals were used as received.

Preparation of sodium hydrogen telluride

An aqueous solution of sodium hydrogen telluride (NaHTe) was prepared based on the method reported for a NaHSe solution (Klayman and Griffin 1973), with some modifications.

Tellurium powder (0.119 g, 0.935mmol) and $NaBH_4$ (0.082 g, 2.17mmol) were loaded into a Schlenk tube. The air was replaced with N_2 by performing freeze-evacuate-thaw cycles. Then, ultrapure water (20 mL), under N_2 atmosphere, was added using a syringe. The mixture was stirred, at 80°C with continuous N_2 flow, until a deep red solution was obtained (45 min). NaHTe solution was used immediately after reaching room temperature.

Synthesis of MAA-coated CdTe quantum dots

CdTe-MAA QDs were synthesized according to a method previously reported in the literature (Gao et al. 1998), with minor modifications.

Briefly, $CdCl_2$(0.037 g, 0.202mmol) was dissolved in ultrapure water (40 mL) and mixed with MAA (0.035 mL, 0.505mmol), in a two necked flask. The pH was adjusted to 10 by addition of 1 M NaOH . Then, the mixture was bubbled with N_2 atmosphere for 30 min .1 .8 mL of freshly prepared NaHTe solution was promptly added to the mixture, using a syringe, at room temperature. The final solution was stirred at 90°C, with continuous N_2 flow, during 6 h , in order to obtain CdTe-MAA QDs with the desired emission wavelength. The reaction was stop by removing the heat source and cooling the reaction with an ice bath. Concentrate solutions of QDs were obtained after 20 min centrifugation with 3500 rpm , using Amicon Ultra-15 centrifugal Filters (3000 MWCO).

Functionalization of quantum dots with 1-dodecanethiol
The highly photoluminescent CdTe-MAA QDs, previously synthetized in aqueous solution, were subject to exchange of the capping ligands according to the strategy described elsewhere (Gaponik et al. 2002).

Briefly, 1 mL of 1-DDT was added on the top of 1 mL of an aqueous solution of CdTe nanoparticles, with a concentration within 4×10^{-3}M range, followed by the addition of 2 mL of acetone. The mixture was stirred and heated to the boiling point of acetone (56 °C). The transfer of the nanoparticles from the aqueous to the organic phase was detected by observing color changes of the latter. CdTe-DDT QDs were separated by decantation, diluted with toluene (1:1) and the nanoparticles precipitated with methanol.

Synthesis of poly (acrylic acid) macroRAFT
Typically, into a 25 mL Schlenk tube, the CTA (0.175 mL , 0.502 mmol) and AA (3.63 g, 50.4mmol) were left to react in the presence of AIBN (0.027 g, 0.164mmol) in THF (2 mL), using the following ratio 1: 0.33: 100 of [CTA]:[AIBN]:[AA]. The mixture was degassed by three freeze-evacuate-thaw cycles and placed under N_2 atmosphere, and the tube was immersed in a thermostatic oil bath at 60°C. After 260 min of polymerization time, the tube was immediately cooled to room temperature. The

reaction mixture was evaporated under reduce pressure and dissolved in a small amount of MeOH . The PAA macroRAFT was precipitated with ethyl ether as a yellow solid. After filtration, the solid was dried in a vacuum oven at room temperature for 24 h . The polymer was dissolved in H_2O and further purified by centrifugation (10,000rpm, 15 min) using 10 kDa Amicon® Ultra-4 Centrifugal Filter Units. PAA macroRAFT was obtained in a conversion degree of 82%. Proton nuclear magnetic resonance (^{1}H NMR) (400 MHz , DMSO- d_6, δ): 0.84(t, $-CH_2CH_3$), 1.22-1.75 [broad m, $-C(CH_3)_2CN$ and CH_2], 2.00-2.40 (broad m, CH, and CH_2), 3.14 (broad m, CH), and 12.22 (broad s, OH). IR (KBr): ν = 3180 (strong), 2930 (medium), 1719 (strong), and 1451 (medium) cm^{-1}.

QDs encapsulation

A fixed amount of CdTe-DDT QDs (0.024 mL , 3.82×10^{-4}M) solution was diluted in chloroform to a final volume of 0.5 mL . Then, it was added to 1 mL of aqueous solution of PAA macroRAFT, with concentration above critical micelle concentration (cmc), accordingly to Table 1. The encapsulation of the QDs was promoted by a 3 min sonication followed by heating the mixture, at 50°C, during 1 h , to completely evaporate the chloroform.

Characterization

Proton nuclear magnetic resonance spectroscopy

The polymer was characterized by ^{1}H NMR spectroscopy in terms of its composition and purity using a 400 MHz Avance Bruker NMR spectrometer equipped with an ultrashield magnet. The ^{1}H NMR chemical shifts are reported in ppm (parts per million). The residual solvent peak has been used as an internal reference. DMSO- d_6 was used as solvent.

Table 1 Amounts of PAA macroRAFT and CdTe-DDT QDs used in the encapsulation assays

PAA macroRAFT (g)	Equivalents	V_{H2O} (mL)	QDs (mL)	V_{CHCl3} (mL)
0.0026	45	1	0.024	0.476
0.0034	60			
0.0172	300			

Fourier transformed infrared spectroscopy

Room temperature infrared spectrum of PAA macroRAFT was recorded on a Jasco spectrometer using transmission mode in the range $4500 - 400\ cm^{-1}$ by averaging 32 scans and using a resolution of 4 cm^{-1}. An amount of 0.020 g of material was mixed with

0.200 g of KBr to prepare the translucent sample disks used in Fourier transformed infrared spectroscopy (FTIR) analysis.

Gel permeation chromatography

PAA macroRAFT solutions (0.1, 0.2, 0.4, 1.0, 2.0, and 5.0mg/mL) were prepared in water and prefiltered on filter plate (hydrophobic polytetrafluoroethylene, 0.45μ m pore size) before injection. The analyses were performed on an Agilent Technologies 1260 Infinity Quaternary Liquid Chromatography System equipped with a standard auto-sampler, thermostatted column compartment, and light scattering, differential refractive index and UV detector.

Differential scanning calorimetry

Thermal properties of PAA macroRAFT were measured using a Perkin Elmer Diamond differential scanning calorimetry (DSC) 131 apparatus, equipped with a LNCS (Liquid Nitrogen Cooling System) accessory. The sample (about 10 mg) was placed in Al pans and heated at 10°C/min from 0 to 140°C, under nitrogen flow. Glass transition temperature (T_g) was taken as the midpoint of the change in heat capacity.

Thermogravimetric analysis

Thermogravimetric measurements were performed in a TA Q500 thermobalance. PAA macroRAFT sample was heated from 40 to 245°C, at 10°C/min under a nitrogen flow (60 mL/min).

Determination of critical micelle concentration

A 100mg/mL stock solution of PAA macroRAFT was prepared in 0.5 M phosphate buffer pH 7.4 . The estimation of the cmc was performed using ANS as fluorescence probe (De Vendittis et al. 1981). A fluorescence spectrum, upon excitation at 350 nm at room temperature, was acquired for solutions with different polymer concentrations, by dilution of the stock solution, and containing 10μM ANS, using a Microplate Reader Synergy MX (Bioteck Instruments).

Photoluminescence measurements

The photoluminescence spectra (PL) of the CdTe QDs were obtained, upon excitation at 360 nm , using a Microplate Reader Synergy MX (Bioteck Instruments). The optical measurements were performed under ambient conditions and the instrumental parameters were kept constant during the characterization.

Photoluminescence quantum yield

The PLQY was determined by comparison of the integrated emission of the QDs samples (λ_{exc} = 360 nm), with that of the standard photoluminescent dye, Rhodamine B, in ethanol (PLQY = 70%) (Arbeloa et al. 1989). It is assumed that solutions of the standard and QDs samples, with similar absorbance (~ 0.022) at the same excitation wavelength, absorb the same number of photons. The PLQYs were calculated based on the following equation:

$$\mathrm{PLQY_f} = \mathrm{PLQY_r} \frac{A_r F_s \eta_s^2}{A_s F_r \eta_r^2} \quad (1)$$

where the subscripts f and r denote test and standard (Rhodamine B) sample, respectively. PLQY is the photoluminescent quantum yield, F corresponds to the integration emission peak area, A stands for the absorbance at excitation wavelength, and η is the refractive index of the solvent.

Electronic microscopy (SEM, TEM, and STEM)

Scanning electron microscopy (SEM) was carried out in a Nova NanoSEM 200 (FEI) equipment, using an acceleration voltage of 15 kV , to analyze the morphology of PAA macroRAFT samples previously coated with a gold thin film.

The morphology and size of the CdTe-DDT QDs were analyzed using transmission electron microscopy (TEM). The ultrasonically dispersed QDs were dropcasted over carbon-coated copper grids, dried, and the micrographs acquired with a JEOL JEM1010 microscope, operating at 100 kV .

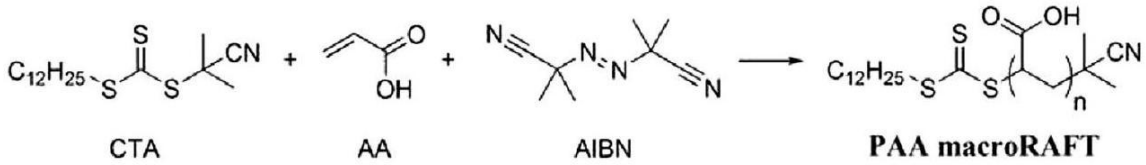

Scheme 1 Synthesis of PAA macroRAFT

Scanning transmission electron microscopy (STEM) assays were performed in order to evaluate the effect of the concentration on the morphology of the polymer aggregates in solution and the entrapment of the QDs by the micelles, with a Nova NanoSEM 200 (FEI) equipment, using an acceleration voltage of 15 kV . The samples were prepared by immersion of copper grids in PAA macroRAFT solutions (1.0, 2.5, and 7.5mg/mL) and in CdTe-DDT QDs encapsulated at different $n_{\mathrm{PAA\ macroRAFT}}/n_{\mathrm{QD}}$ ratios (45, 60, and 300), followed by drying at room temperature.

Results and discussion

PAA macroRAFT is a surfactant homopolymer that was designed to be produced in a single chemical reaction. Its synthesis was based on the RAFT polymerization of AA in the CTA, 2-cyano-2-propyl dodecyl trithiocarbonate, in the presence of AIBN, which resulted in an

82% conversion degree (Scheme 1). The chemical structure of the resulting material was confirmed by ^{1} H NMR and FTIR analyses. The ^{1}H NMR spectrum exhibits NMR resonances typical of aliphatic protons, assigned in the range of 0.84 to 3.14 ppm , and a broad
resonance, at 12.22 ppm , typical of hydroxyl protons of the carboxylic acid group. The FTIR spectrum reveals the presence of the carboxylate function, since it displays a $0-C=0$ stretch band at 1719 cm^{-1}, the stretch of aliphatic C-H at 2923 cm^{-1} and a broad signal above 3000 cm^{-1} associated to the hydrogen-bonded $0-H$ stretch of -COOH .

Thermal properties of PAA macroRAFT (Fig. 1) were determined by DSC and thermogravimetric analysis (TGA). The T_g of approximately 120°C, measured by DSC, is in agreement with other values reported in literature (Al-Najjar et al. 1996; Dubinsky et al. 2004). A full TGA characterization was not possible, due to the fact that, by increasing the temperature above 245°C, the residue expands and sticks to the oven plate. Nevertheless, it was possible to observe the degradation step of trithiocarbonate at 133 °C and the start of chain scission reaction of PAA that usually occurs at 180°C (Zhang et al. 2003). Both analyses confirmed that PAA macroRAFT was efficiently synthesized.

Gel permeation chromatography (GPC) assays were performed in order to determine the molecular weight of PAA macroRAFT. Figure 2 depicts the normalized GPC chromatograms of PAA macroRAFT, acquired using solutions with different polymer concentrations. For

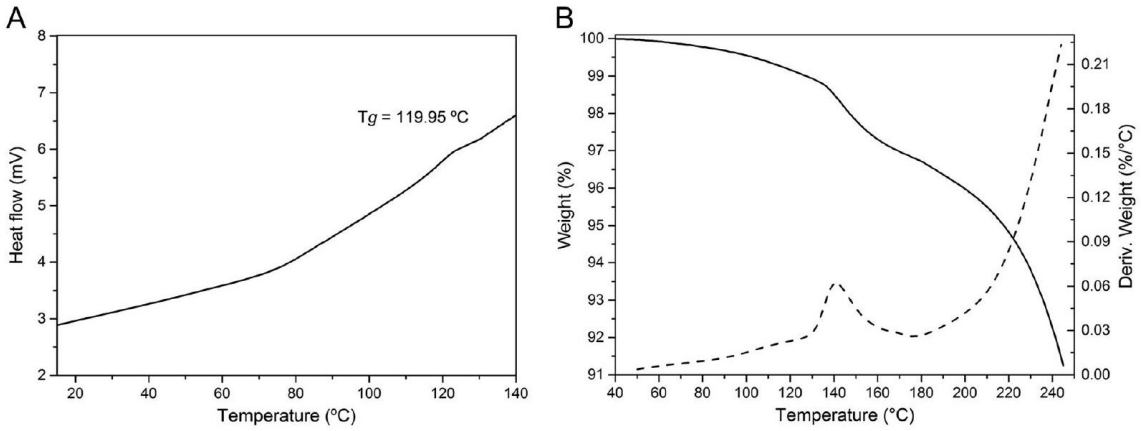

Fig. 1 DSC (a) and TGA (b) thermograms of PAA macroRAFT

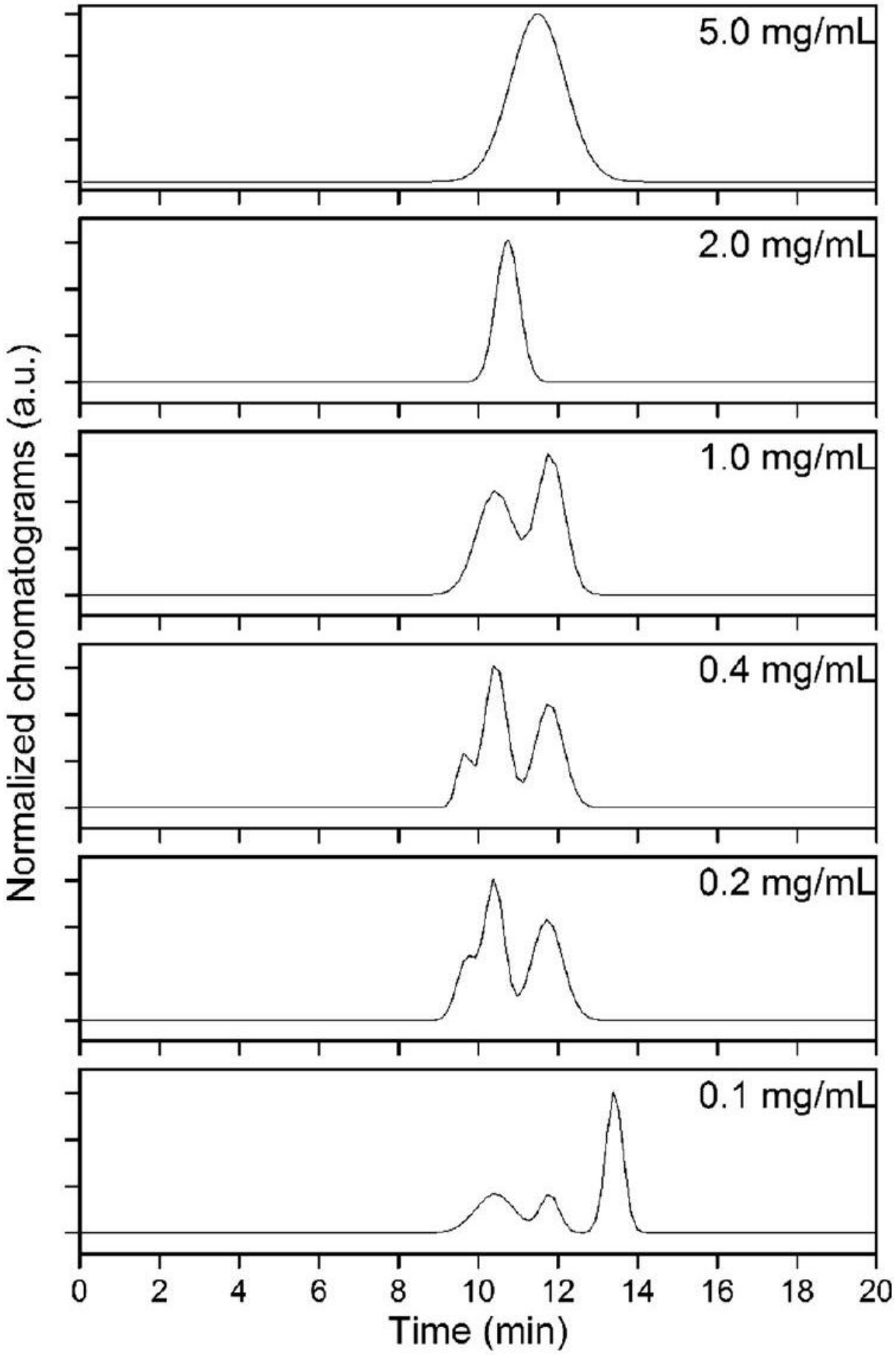
5.0 mg/mL
2.0 mg/mL
1.0 mg/mL
0.4 mg/mL
0.2 mg/mL
0.1 mg/mL
Normalized chromatograms (a.u.)
0
2
4
6
8
10
12
14
16
18
20
Time (min)

Fig. 2 Normalized GPC chromatograms of PAA macroRAFT

5.0 and 2.0mg/mL, it is possible to observe the presence of only one peak, consistent with the presence of only one species in both solutions. Nevertheless, the number average molecular weight (M_n) and molecular weight (M_w) obtained with these GPC chromatograms (Table 2) were higher than the theoretical ones. It is expected that PAA macroRAFT could form supramolecular aggregates, such as micelles, in solution. If that is the case, the M_n and M_w would be increased when compared to the predicted ones, supporting the observations. This fact was already observed for other systems capable of forming such aggregates (Yokoyama et al. 1993). Decreasing the polymer concentration leads to the detection of several peaks in the chromatogram, due to the presence of aggregates with different sizes. This confirms that PAA macroRAFT is able to form supramolecular aggregates. It was also observed that these aggregates start to form below 0.1mg/mL and reach their maximum size above 2.0mg/mL. Below this concentration, the peaks' overlay does not allow an accurate determination of the M_n and M_w, and for that reason, the values were not presented.

$M_n($ theo $) = \frac{W_M}{\left(\frac{W_{CTA}}{M_{WCTA}}\right)} x$ conversion $+ M_{WCTA}$

where W_M and W_{CTA} are the weight of AA and CTA respectively, M_{wCTA} is the molecular weight of the CTA.

Although the GPC data already showed that micellar systems based on PAA macroRAFT were successfully accomplished, it was essential to determine the cmc, concentration at which micelles of our material start to form (Gohy 2005). This parameter is difficult to determine with accuracy for polymeric surfactants using the common methods applied for LMWS (Ahmad et al. 2014). Nevertheless, fluorimetric assays based on fluorescence probes sensitive to the polarity give reliable results (De Vendittis et al. 1981; Kwon et al. 1993). The cmc of PAA macroRAFT was determined by a fluorimetric study of aqueous solutions of the polymer containing a fluorescent probe, 8-anilino-1-naphthalenesulfonic acid (ANS) (Birdi et al. 1979; de Sá et al. 2010; De Vendittis et al. 1981). It was acquired the ANS's fluorescence emission spectra in the presence of several

Table 2 Parameters obtained by GPC analysis of PAA macroRAFT and calculated using Eq. 2

[a] Gravimetric yield

[b] Not determined

Concentration (mg/mL)	Conversion (%) [a]	M_n (theo) (g/mol)	M_n (exp) (g/mol)	M_w (exp) (g/mol)	PDI
0.1	82	6310	_ [b]	[b]	[b]
0.2			_b	_b	_b
0.4			_ [b]	_b	_b
1.0			1.1×10^4	2.6×10^4	2.5
2.0			3.1×10^4	1.8×10^5	5.7
5.0			6.5×10^4	1.5×10^5	2.3

Fig. 3 Normalized fluorescence intensity of the ANS at 430 nm , upon excitation at 350 nm , as function of the PAA macroRAFT concentration. The intersection of the linear least-square fitting curves corresponds to the critical micelle concentration

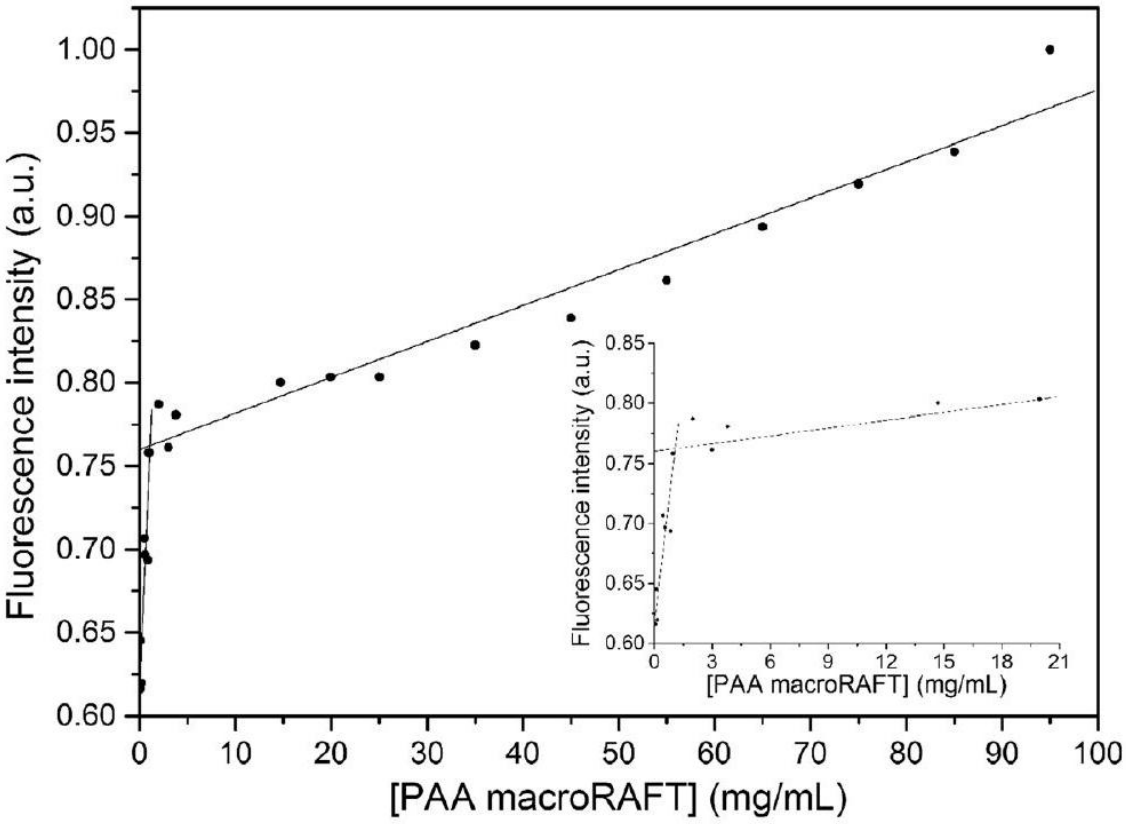

polymer concentrations. For higher values, it was observed a shift in the ANS' emission wavelength from the expected 480 nm to the range of 430 to 440 nm . Moreover, as the concentration increases, the fluorescence intensity also increases. Thus, this fact was attributed to the internalization of ANS into the micelles' core. The fluorescence intensity of ANS was plotted as function of the PAA macroRAFT concentration, and the cmc, 2.08mg/mL, was determined by a linear leastsquare fitting analysis (Fig. 3).

Even though MAA already promotes water solubility, QDs capped with small thiol molecules may have lower photostability (Aldana et al. 2001). Taking that into account, the capping ligand was exchanged, MAA by DDT, and restored the water solubility by entrapping
the QDs in micelles. A fixed amount of CdTe-DDT QDs (0.024 mL, 3.82×10^{-4}M) solution was diluted in chloroform to a final volume of 0.5 mL , which was added to 1 mL of aqueous solution of PAA macroRAFT, with concentration above cmc(2.08mg/mL), according to Table 1. The encapsulation of the QDs was promoted by a 3 min sonication followed by heating the mixture, at $50\ ^{\circ}$C, during 1 h to complete evaporate the chloroform.

SEM analysis (Fig. 4) of PAA macroRAFT revealed that the polymer does not form particles with welldefined structure. Additionally, it was observed that the beam caused modifications on its morphology, suggesting that it is a very hygroscopic polymer. STEM

analyses (Fig. 5) were performed for solutions of PAA

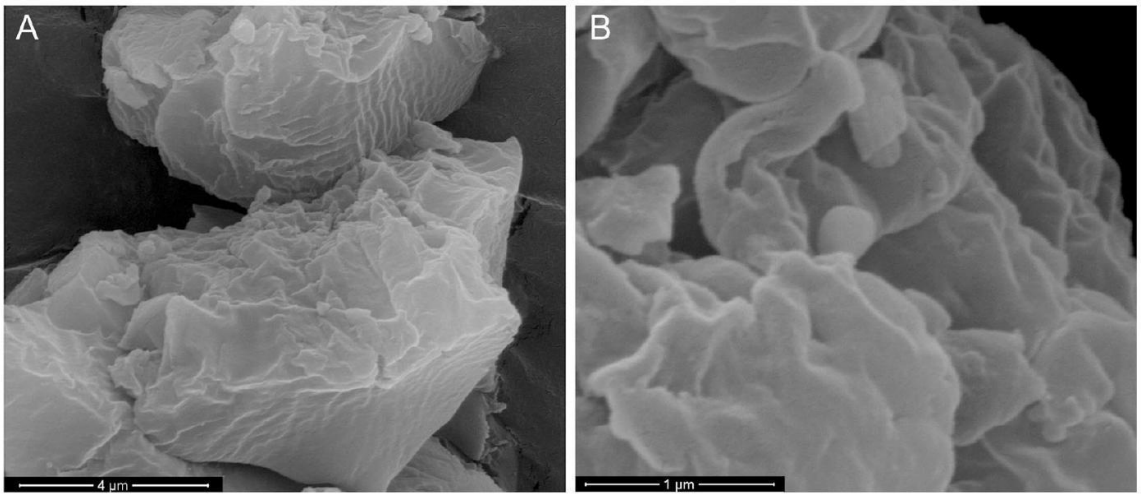

Fig. 4 SEM micrographs of PAA macroRAFT at different magnification

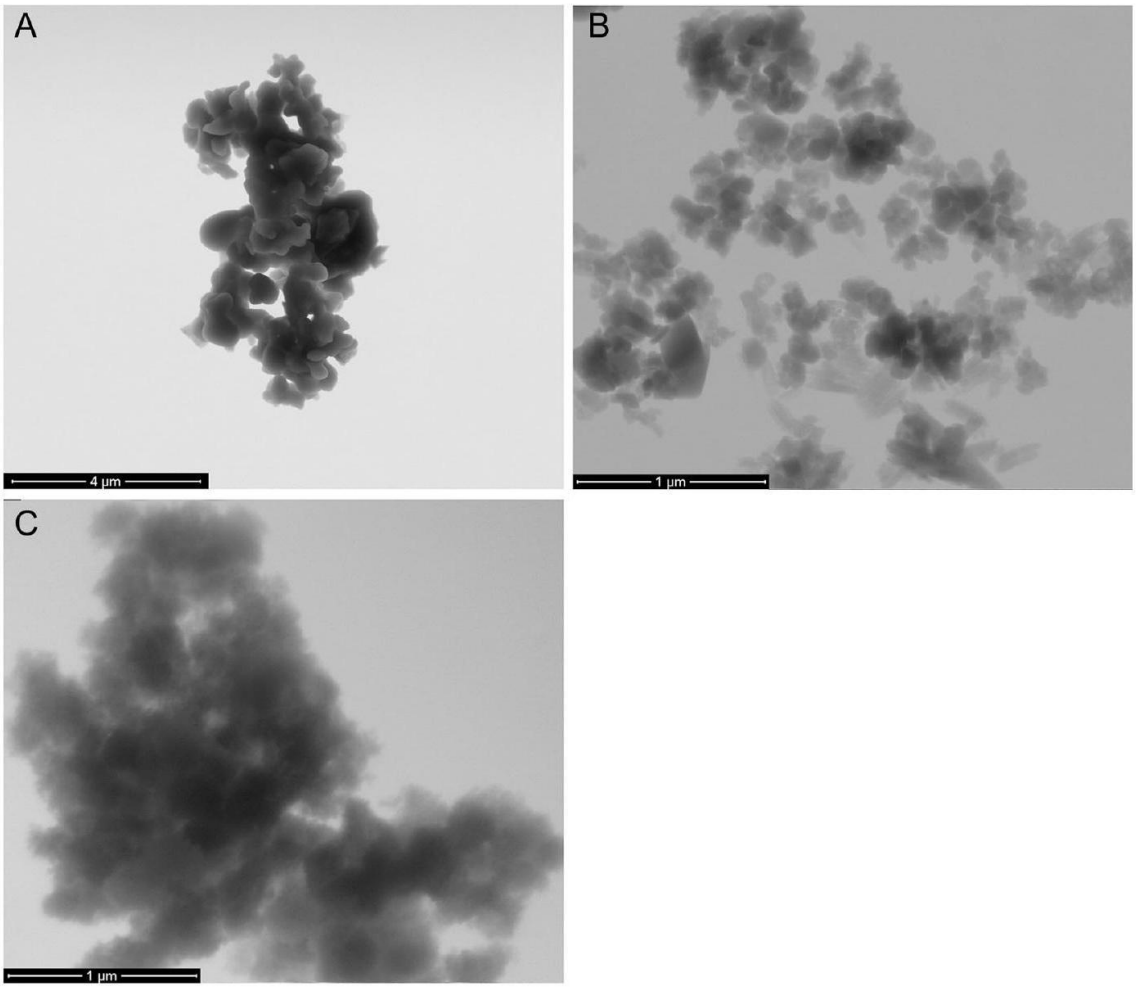

Fig. 5 STEM micrographs of PAA macroRAFT aqueous solutions at 1.0mg/mL(a),2.5mg/mL(b), and 7.5mg/mL(c) macroRAFT with different concentrations, in order to understand the influence of micelle formation on the particles' morphology. Thus, samples with concentration below cmc(1.0mg/mL), near the cmc(2.5mg/mL),

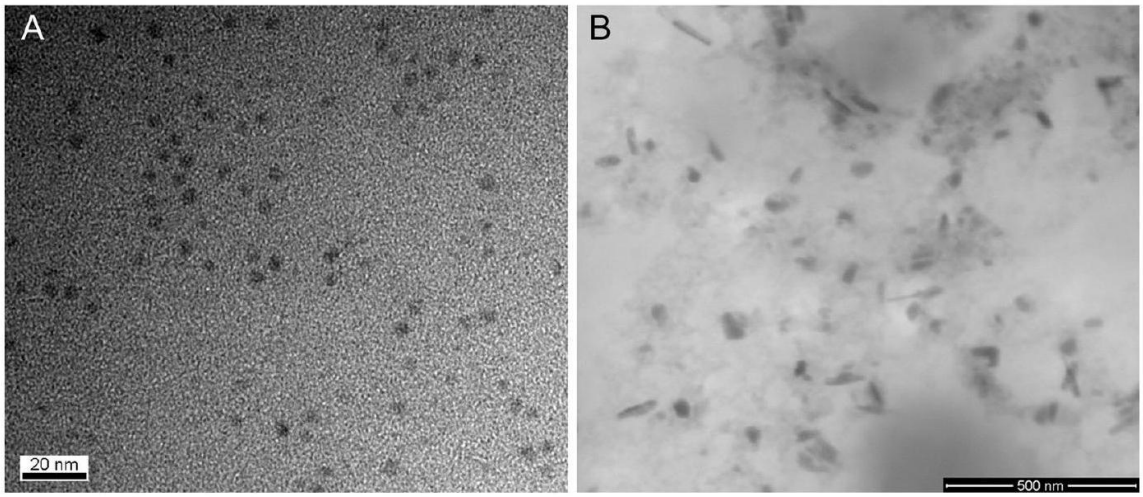

Fig. 6 TEM micrograph of CdTe-DDT QDs (a) and STEM micrograph CdTe-DDT entrapped by PAA macroRAFT with $n_{\text{PAA macroRAFT}}$ / n_{QD} ratio of 45 (b)

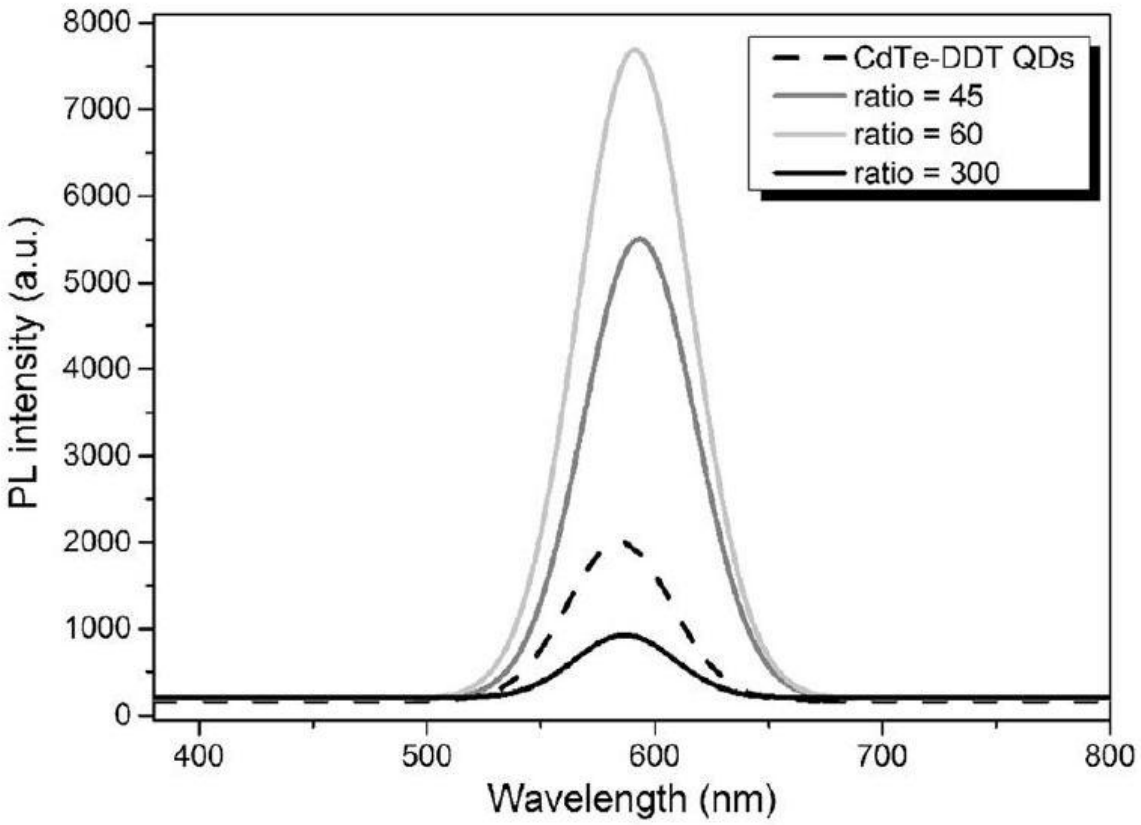

Fig. 7 PL emission spectra ($\lambda_{ex} = 360$ nm) of the original CdTeDDT QDs and encapsulated by PAA macroRAFT

and well above cmc (7.5mg/mL) were studied. It could be noticed that, as the concentration increases, PAA macroRAFT tend to form smaller spherical particles, with less dispersed sizes. This is in agreement with the GPC observations, in which was possible to identify several species in solution below and at cmc, while above cmc the presence of only one signal supports the particle size homogeneity. Below cmc, hydrogen bonds should predominate in the interactions between molecules, allowing a less restrict interaction, when compared to what happens in micelles, forming larger aggregates. As the concentration increases, Van der Waals forces and hydrogen bonds became responsible for micelle formation, restricting the interactions between molecules to their surroundings, in well-defined structures. However, at cmc, the polymer is not completely aggregated into micelles, and different structures could be found. Above cmc, micelles with welldefined structure are completely formed, being the structures that prevail in solution.

Figure 6a depicts the TEM micrograph of CdTe DDT QDs. As it can be noticed, CdTe QDs are welldispersed, with nearly spherical shape, without aggregation and with a size around 3.5 nm , which is the same size that was obtained following the Yu et al. (2003) methodology. The encapsulation by PAA macroRAFT micelles ($n_{\text{PAA macroRAFT}}/n_{\text{QD}}$ ratio of 45 , 60, and 300) affects the QDs' dispersion, with smaller impact with lower ratio. Figure 6b depicts the STEM micrograph of the system with the 45 ratio, in which is possible to observe QDs clusters with size around 100 nm . One possible explanation for this behavior could be related with the limited mobility of the QDs

when being transferred, by entrapment, from the organic phase to the aqueous medium, due to the high micelles concentration.

Increasing the $n_{\text{PAA macroRAFT}}/n_{\text{QD}}$ ratio to an optimal value reduces the aggregation of QDs encapsulated by the micelles and, therefore, suppresses the possible aggregation-induced quenching of QDs (Zhu et al. 2015). Figure 7 shows the effect of the amount of PAA macroRAFT on the PL intensity of the polymercoated QDs. The lower $n_{\text{PAA macroRAFT}}/n_{\text{QD}}$ ratios of 45 and 60 afforded the better results of PL, being the higher PL obtained with the ratio of 60. The larger aggregates obtained using the higher $n_{\text{PAA macroRAFT}}/n_{\text{QD}}$ ratio (300) resulted in a decrease of the PL intensity due to self-quenching (Zhu et al. 2015). These results showed that it is important to keep an optimal molar ratio of PAA macro RAFT/QDs to enhance the QDs PL intensity, which was associated to an approximately 23% enhancement of the PLQY. An enhancement of PL was also observed by Yuwen et al. (2011) and Haibing et al. (2007) when they entraped different QDs, respectively CdTe/CdS and CdSe/ZnS core/shell QDs , in micelles.

Conclusions

The surfactant homopolymer PAA macroRAFT was successfully synthetized by RAFT polymerization with high conversion yield. Its surfactant behavior was studied by fluorimetric measurements based on the influence of the polarity on the ANS' fluorescence (de Sá et al. 2010; De Vendittis et al. 1981). The micelles formation and morphology were also studied by GPC and STEM assays.

The entrapment of hydrophobic quantum dots in the inner part of micelles is a useful method to stabilize them and improve their optical properties (Yuwen et al. 2011). Based on these facts, we have entrapped hydrophobic CdTe-DDT QDs in PAA macroRAFT micelles in order to solubilize them in water. In another system (Yuwen et al. 2011), the ratio between surfactant and QDs showed to be of high importance to the QDs' optical properties. For that reason, CdTe-DDT QDs were entrapped by PAA macroRAFT with different proportions (45, 60, and 300 equivalents). The systems prepared were studied by STEM and fluorimetric assays. It was observed that the amount of PAA macroRAFT induces morphology alterations to the QDs and influences their photoluminescence. A 23% enhancement of the PLQY was achieved when our CdTe-

DDT QDs were stabilized using 60 equivalents of PAA macroRAFT.

Our findings prove the effectiveness of this methodology to prepare stable and high photoluminescent polymercoated QDs in aqueous solution, thus, offering a new opportunity for testing our materials as light harvesting agents, based on energy transfer phenomena (Clapp et al. 2005). Considering the developed system as energy acceptor in a fluorophore pair able to experience energy transfer phenomena, it could be combined with a suitable energy donor, whose emission spectrum overlaps the absorption spectrum of the QDs in the range $500 - 550$ nm; thus, it would be possible to develop a new system for such purpose.

Acknowledgements The authors acknowledge n-STeP-Nanostructured systems for Tailored Performance, with reference NORTE-07-0124-FEDER-000039, supported by the Programa Operacional Regional do Norte (ON.2), PEst-C/CTM/ LA0025/2013 (Strategic Project-LA 25-2013-2014).

References

Ahmad Z, Shah A, Siddiq M, Kraatz H-B (2014) Polymeric micelles as drug delivery vehicles. RSC Adv 4:1702817038. doi:10.1039/C3RA47370H

Aldana J, Wang YA, Peng X (2001) Photochemical instability of CdSe nanocrystals coated by hydrophilic thiols. J Am Chem Soc 123:8844-8850. doi:10.1021/ja 016424q
Al-Najjar MM, Hamid SH, Hamad EZ (1996) The glass transition temperature of nitrated polystyrene/poly (acrylic acid) blends. Polym Eng Sci 36:2083-2087. doi:10.1002/pen. 10604
Arbeloa FL, Ojeda PR, Arbeloa IL (1989) Flourescence selfquenching of the molecular forms of Rhodamine B in aqueous and ethanolic solutions. J Lumin 44:105-112. doi:10.1016/0022-2313(89)90027-6
Birdi KS, Singh HN, Dalsager SU (1979) Interaction of ionic micelles with the hydrophobic fluorescent probe 1-anilino-8-naphthalenesulfonate. J Phys Chem 83:2733-2737. doi:10.1021/j100484a010
Clapp AR, Medintz IL, Fisher BR, Anderson GP, Mattoussi H (2005) Can luminescent quantum dots be efficient energy acceptors with organic dye donors? J Am Chem Soc 127: 1242-1250. doi:10.1021/ja 045676z
de Sá A, Prata MIM, Geraldes CFGC, André JP (2010) Triaza-based amphiphilic chelators: synthetic route, in vitro characterization and in vivo studies of their Ga (III) and Al (III) chelates. J Inorg Biochem 104:1051-1062. doi:10.1016/j.jinorgbio. 2010.06.002

De Vendittis E, Palumbo G, Parlato G, Bocchini V (1981) A fluorimetric method for the estimation of the critical micelle concentration of surfactants. Anal Biochem 115:278-286. doi:10.1016/0003-2697(81)90006-3
Dubinsky S, Grader GS, Shter GE, Silverstein MS (2004) Thermal degradation of poly (acrylic acid) containing copper nitrate. Polym Degrad Stab 86:171-178. doi:10.1016/j. polymdegradstab. 2004.04.009
Gao M, Kirstein S, Möhwald H, Rogach AL, Kornowski A, Eychmüller A, Weller H (1998) Strongly photoluminescent CdTe nanocrystals by proper surface modification. J Phys Chem B 102:8360-8363. doi:10.1021/jp9823603
Gaponik N, Talapin DV, Rogach AL, Eychmuller A, Weller H (2002) Efficient phase transfer of luminescent thiol-capped nanocrystals: from water to nonpolar organic solvents. Nano Lett 2:803-806. doi:10.1021/n1025662w
Gohy J-F (2005) Block copolymer micelles. In: Abetz V (ed) Block copolymers II. Springer, Berlin
Haibing L, Xiaoqiong W, Zhinong G, Zhike H (2007) Gemini surfactant for fluorescent and stable quantum dots in aqueous solution. Nanotechnology 18:205603. doi:10.1088/09574484/18/20/205603
Hoffman JB, Choi H, Kamat PV (2014) Size-dependent energy transfer pathways in CdSe quantum dot-squaraine lightharvesting assemblies: Förster versus Dexter. J Phys Chem C 118:18453-18461. doi:10.1021/jp506757a
Klayman DL, Griffin TS (1973) Reaction of selenium with sodium borohydride in protic solvents. A facile method for the introduction of selenium into organic molecules. J Am Chem Soc 95:197-199. doi:10.1021/ja00782a034
Kwon G, Naito M, Yokoyama M, Okano T, Sakurai Y, Kataoka K (1993) Micelles based on AB block copolymers of poly(ethylene oxide) and poly(β-benzyl L-aspartate). Langmuir 9: 945-949. doi:10.1021/la00028a012
Ramachandra S, Popović ZD, Schuermann KC, Cucinotta F, Calzaferri G, De Cola L (2011) Förster resonance energy transfer in quantum dot-dye-loaded zeolite L. Nanoassemblies

Small 7: 1488-1494. doi:10.1002/smll.201100010
Snaith HJ (2013) Perovskites: the emergence of a new era for lowcost, high-efficiency solar. Cells J Phys Chem Lett 4:36233630. doi:10.1021/jz4020162

Viet Ha C, Thi Ha Lien N, Tien Ha L, Dinh Lam V, Hong Nhung T, Thi Kim Lien V (2012) Synthesis and optical properties of water soluble CdSe/CdS quantum dots for biological applications. Adv Nat Sci Nanosci Nanotechnol 3:025017. doi:10.1088/2043-6262/3/2/025017
Yokoyama M, Sugiyama T, Okano T, Sakurai Y, Naito M, Kataoka K (1993) Analysis of micelle formation of an adriamycinconjugated poly(ethylene glycol)-poly (aspartic acid) block copolymer by gel permeation chromatography. Pharm Res 10:895-899. doi:10.1023/A:1018921513605
Yu WW, Qu L, Guo W, Peng X (2003) Experimental determination of the extinction coefficient of CdTe. CdSe CdS Nanocrystals Chem Mater 15:2854-2860. doi:10.1021/cm 034081k
Yu WW, Chang E, Drezek R, Colvin VL (2006) Water-soluble quantum dots for biomedical applications. Biochem Biophys Res Commun 348:781-786. doi:10.1016/j.bbrc. 2006.07.160
Yuwen L et al (2011) One-pot encapsulation of luminescent quantum dots synthesized in aqueous solution by amphiphilic. Polymers Small 7:1456-1463. doi:10.1002/smll. 201002039

Zhang H et al (2003) From water-soluble CdTe nanocrystals to fluorescent nanocrystal-polymer transparent composites using polymerizable surfactants. Adv Mater 15:777-780. doi:10.1002/adma. 200304521
Zhou D, Lin M, Chen Z, Sun H, Zhang H, Sun H, Yang B (2011) Simple synthesis of highly luminescent water-soluble CdTe quantum dots with controllable surface functionality. Chem Mater 23:4857-4862. doi:10.1021/cm 202368w
Zhu Z et al (2015) Stable and size-tunable aggregation-induced emission nanoparticles encapsulated with nanographene oxide and applications in three-photon fluorescence. Bioimaging ACS Nano:10. doi:10.1021/acsnano.5b05606